Determination of the Water–Gas Shift Reaction and Catalyst Deactivation Kinetics from Non-Isothermal Fixed Bed Reactor Data*

Riita L. Keiski,[a,†] Tapio Salmi[b] and Veikko J. Pohjola[a]

[a]Department of Process Engineering, University of Oulu, SF-90570 Oulu and [b]Department of Chemical Engineering, Åbo Akademi, SF-20500 Turku, Finland

Keiski, R. L., Salmi, T. and Pohjola, V. J., 1990. Determination of the Water–Gas Shift Reaction and Catalyst Deactivation Kinetics from Non-Isothermal Fixed Bed Reactor Data. – Acta Chem. Scand. 44: 777–783.

The water–gas shift reaction over a commercial iron oxide/chromium oxide catalyst was investigated to elucidate the reaction and the catalyst deactivation kinetics as well as the physical properties of the catalyst. A non-isothermal laboratory scale fixed bed reactor operating close to industrial practice was used in all experiments. The reactor feed temperature was varied between 575 and 675 K and the water-to-dry gas ratio was between 0.33 and 1.24.

The catalyst activity decayed rapidly during the first 150 h of operation, after which the decay became much slower. The slow decline of the activity was found to be due to a sintering process: a decrease of the surface area and a growth of the mean pore size.

The kinetic experiments performed at atmospheric pressure during the slow decay of the catalyst activity showed that the reaction rate is strongly dependent on the CO concentration, moderately dependent on the H_2O concentration and weakly dependent on the CO_2 concentration and practically independent of the H_2 concentration. The kinetic and deactivation parameters were determined by nonlinear regression using the temperature and conversion profiles of the catalyst bed. The following rate equation was obtained: $r = k' c_{CO}^{0.74} c_{H_2O}^{0.47} c_{CO_2}^{-0.18} (1-\beta)$ where $k' = 2.6234\times10^6 \exp(-9598/T)$ $(dm^3)^{1.03}$ $mol^{-0.03}$ kg^{-1} s^{-1} and the factor β accounts for the reversibility: $\beta = c_{CO_2}c_{H_2}/(c_{CO}c_{H_2O}K)$, where K is the equilibrium constant. The time dependence of the catalyst activity was included in the rate constant using a hyperbolic model $k' = A_0[1/(1+at)]$ where $A_0 = 5.0494\times10^6$ $(dm^3)^{1.03}$ $mol^{-0.03}$ kg^{-1} s^{-1} and $a = 2.9293\times10^{-3}$ h^{-1}.

The water–gas shift reaction, reaction (1), is applied to produce hydrogen, e.g. for ammonia synthesis, to adjust the H_2-to-CO mole ratio of the synthesis gas, and to detoxify town gases.[1,2]

$$CO + H_2O = CO_2 + H_2$$

$$\Delta H(298\ K) = -41.09\ kJ\ mol^{-1} \qquad (1)$$

$$\Delta S(298\ K) = -42.39\ J\ K^{-1}\ mol^{-1}$$

Iron oxides were among the earliest shift catalysts used industrially. They operate in the temperature range 320–450 °C. These high-temperature catalysts usually contain chromium oxide as a stabilizer to retard sintering and loss of surface area. The catalytically active component is, however, magnetite, which is formed by a reduction of Fe_2O_3 to Fe_3O_4 in process conditions.

During recent years, numerous studies of the reaction kinetics over iron oxide/chromium oxide catalysts have been reported. There is, however, little agreement on the precise form of the rate equation or the values of the rate constants. Both first-order[3] and second-order[4] kinetics have been suggested, but many other more complex rate equations have also been proposed.[5–9]

The iron oxide/chromium oxide catalyst loses its activity in use. According to experiences from laboratory experiments as well as in commercial shift reactors, the catalyst activity is initially very high during the first 100–150 h of operation, but it decreases gradually with time. The activity decrease is quite rapid between 150 and 400 h, and comparatively slower between 400 and 700 h, after which the activity is practically steady up to 1000 h.[10,11] Sintering or ageing of the iron oxide/chromium oxide catalyst is reported[3,4,9,12,13] to be the main reason for the decline of the catalytic activity. Sintering lowers the surface area, reduces the porosity, increases the particle size and decreases the number of small pores (diameter <30 nm).[11]

Catalytic kinetics are often studied in gradientless test reactors. However, the most common catalytic reactor is a fixed bed. The aim of the present work is to illustrate the use of a non-isothermal fixed bed reactor in determination of the shift reaction kinetics and catalyst deactivation.

*Presented at the 2nd Nordic Symposium on Catalysis, Lyngby, Denmark, November 2–3, 1989.

†To whom correspondence should be addressed.

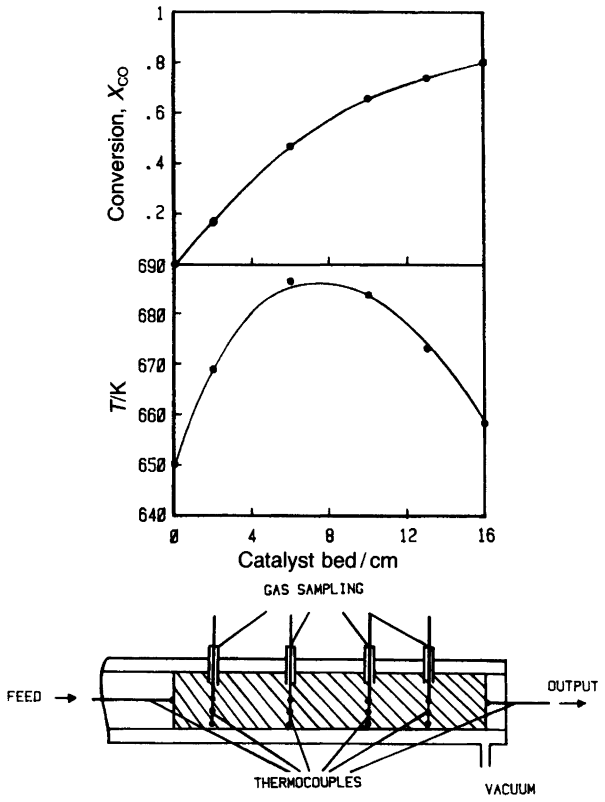

Fig. 1. Outline of measurement.

Experimental

Experimental conditions corresponding to industrial practice were used in the kinetic studies: the inlet temperature was varied between 575 and 675 K, the water-to-dry gas ratio was between 0.33 and 1.24, and the dry gas contained typically 7–30 % CO, 3–20 % CO_2 and 25–70 % H_2, the rest being N_2. Cylindrical iron oxide/chromium oxide catalyst particles (Catalysts & Chemicals Europe) of size 3.2×3.2 mm were used.

The kinetic experiments were performed at atmospheric pressure during the slow decay of the catalyst activity. The equipment used in the kinetic studies comprised a gas flow regulation and mixing system, a reactor section and an on-line analytical section. A detailed description of the reactor system is given elsewhere.[14] Experiments were performed by changing the inlet temperature, the H_2O-to-dry gas mole ratio and the CO, CO_2 and/or H_2 concentrations in the reaction gas. The bed temperature was measured and the reaction gas samples were taken at six axial positions (Fig. 1).

The stability of the catalyst was studied by repeating a set of experiments after certain time periods. Experiments using N_2 adsorption at −196 °C and Hg porosimetry[15–17] were made to investigate the changes in the catalyst surface area, pore distribution, total pore volume and average pore radius during the process. XPS studies were made to determine the surface compositions of one fresh and some used catalysts.

Results

Reaction kinetics. The kinetic parameters were determined using the plug flow model. Thus, the continuity equation for carbon monoxide is given by eqn. (2), where $\dot{n}_{CO}$ is the molar flow of CO.

$$d\dot{n}_{CO}/dV = r_{CO}\varrho_b \qquad (2)$$

The rate expression in eqn. (2) was assumed to be of the power law type, eqn. (3), where β is the reversibility factor: $\beta = c_{CO_2}c_{H_2}/)Kc_{CO}c_{H_2O})$ and $k = k' \exp(-E/RT)$.

$$-r_{CO} = kc_{CO}^n c_{H_2O}^m c_{CO_2}^p c_{H_2}^q (1-\beta) \qquad (3)$$

The non-isothermal approach in parameter estimation requires data on carbon monoxide conversion and reaction temperature vs. catalyst bed length, as shown in Fig. 1. The axial temperature profile was approximated by an empirical fourth-order polynomial to avoid the use of the energy balance during the estimation of the kinetic parameters. The radial temperature profiles were neglected, since they were within the experimental error.

Twelve experimental runs with inlet temperatures between 600–750 K and with catalyst ages between 212–251 h were chosen for the parameter estimation study. These data cover the concentration domain well, since the extreme inlet concentrations of the gas components are included.

The kinetic parameters in eqn. (3) were estimated stepwise using a non-linear regression program REPROCHE.[18] In the first step, k' and E were estimated (the two-parameter model) keeping m, p and q fixed at 0 and n at 1. In the

Table 1. Estimation of the parameters in the power-law rate equation.

No. of parameters	$\ln(k')^a$	s/%	E/R^b	s/%	n	s/%	m	s/%	p	s/%	$MRS\times10^a$
3	13.30	1.8	9243	2.5	0.77	3.3	–	–	–	–	0.17
4	15.93	1.4	9407	1.7	0.73	2.5	0.55	7.6	–	–	0.08
5	14.78	1.9	9598	1.8	0.74	2.5	0.47	10.1	−0.18	25.	0.08

[a]Units $(dm^3)^{n+m+p+q}\ kg^{-1}\ s^{-1}\ mol^{-(n+m+p+q-1)}$. [b]Units K.

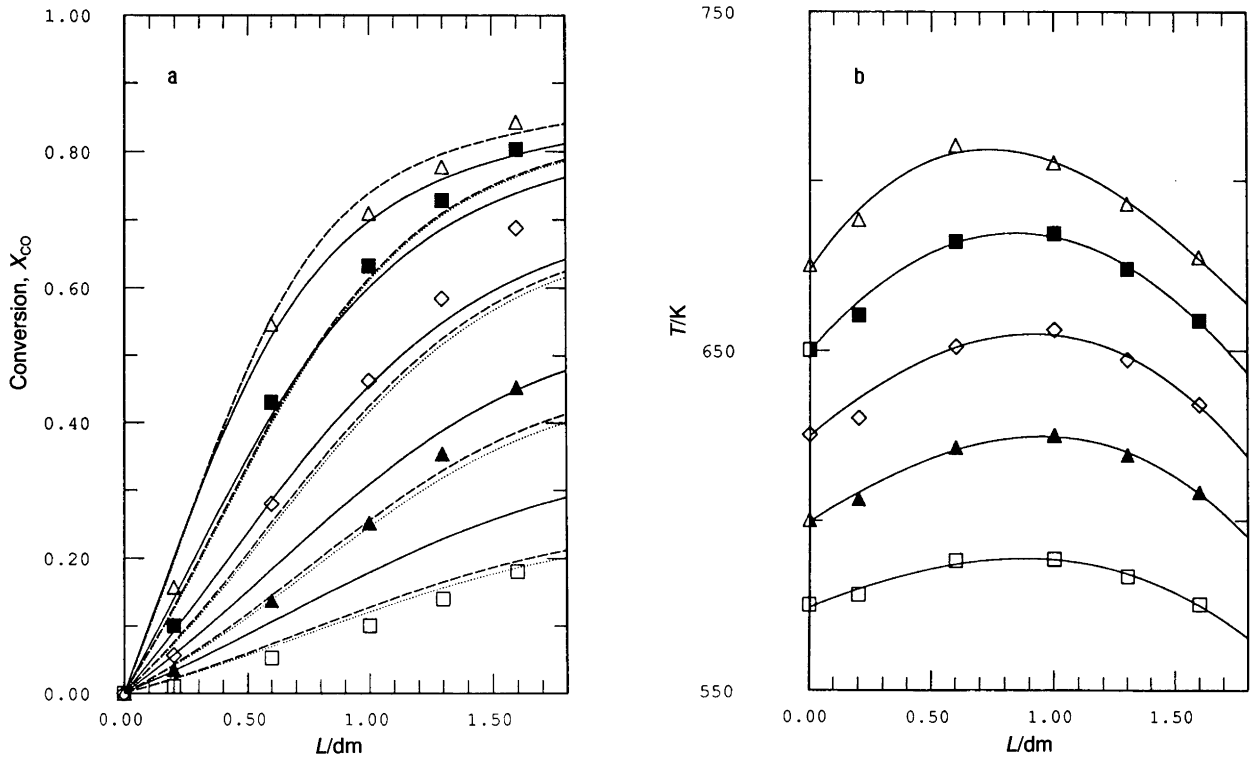

Fig. 2. (a) The model predictions compared to independent conversion data; (——) two-parameter model, (···) three-parameter model, (– – –) four-parameter model. (b) Temperature profiles corresponding to the experiments in (a). (□) $T_0 = 600$ K, (▲) $T_0 = 600$ K, (◇) $T_0 = 625$ K, (■) $T_0 = 650$ K, (△) $T_0 = 675$ K and the inlet conditions: $\dot{n}_{0,CO} = 1.1$ mol h^{-1}, $S = 1997$ h^{-1}, the inlet mole ratios: H_2O/CO = 6.1, CO_2/CO = 0.67, H_2/CO = 4.0.

following steps, three parameters (k', E and n) and four parameters (k', E, n and m) were determined (the three- and four-parameter models), and in the final stage all five parameters (k', E, n, m and p) were determined simultaneously (the five-parameter model). The H_2 concentration exponent (q) was always kept zero because the effect of the H_2 concentration was negligible on the forward shift reaction. The observed and estimated conversions were finally compared by solving the differential equation using a semi-implicit Runge–Kutta method.[19]

The results of the regression analysis are given in Table 1. The results from the three- and four-parameter models are quite similar. The activation energy is 77–78 kJ mol^{-1} and the concentration exponent of CO is between 0.7 and 0.8 according to both models. The water concentration exponent (m) becomes less accurate, since water was present in most experiments in a quite large excess: the H_2O-to-CO ratio varied between 2.7 and 12.0. The standard deviation of the CO concentration exponent is about 2–3 %, whereas that of the H_2O exponent is about 7 %. The inclusion of the fifth parameter (p) in the model did not essentially improve the overall fit, and the mean residual square remained on the same level. A small negative value ($p = -0.18$) indicates the inhibitory effect of CO_2 on the reaction rate. The results concerning the activation energy and the exponents of the potency law kinetic equation [eqn. (3)] are in fairly good agreement with the data presented in the literature.[4,12,20–23]

The computed conversion profiles using the two-, three- and four-parameter models are shown in Fig. 2a. The corresponding temperature profiles are given in Fig. 2b. The comparison of the computed and the experimental conversion profiles indicates that the rate model suggested describes the reactor behaviour well. The reactor performance can be predicted by the three- and four-parameter models within the whole temperature domain. A more extensive comparison of the experimental and computed conversion profiles revealed that the plug flow model is sufficient to describe the reactor flow pattern, since the model seems to be valid within a large temperature, space velocity and concentration interval.[14]

Deactivation. The catalyst stability was determined by measuring the conversion and temperature profiles along the reactor at different times of operation. Between these time points, reaction conditions were changed (changes in the inlet temperature, component concentration and H_2O-to-dry gas ratio).

A fast decline in the catalyst activity was detected during the first 150 h of operation, after which the decay became

Table 2. Estimation of the parameters in the rival deactivation models.

Experiment	A_0[a]	s/%	a[b]	s/%	$MRS\times10^{-10}$
$k' = A_0\exp(-at)$					
A10	3571500	1.91	0.0022824	5.00	0.568185
B12	4739700	1.87	0.0020881	4.94	0.337200
C12	4465700	4.98	0.0014065	18.19	3.31120
D12	4835000	5.05	0.0019299	14.98	10.4223
$k' = A_0[1/(1+at)]$					
A10	3991000	2.32	0.0040609	6.43	0.331304
B12	5100700	2.17	0.0032197	6.15	0.228233
C12	4720000	5.69	0.0020856	21.40	2.37636
D12	5186700	4.71	0.0031400	15.47	5.95739
$k' = A_0[1/(1+at)]^2$					
A10	3747400	1.93	0.0014811	5.24	0.389513
B12	4895800	1.94	0.0012717	5.33	0.268901
C12	3577400	5.26	0.0008438	19.58	2.83308
D12	499760	4.89	0.0012154	15.29	8.08488
$k' = A_0[1/(1+at)]^3$					
A10	3683200	1.90	0.0009009	5.10	0.434378
B12	4839500	1.91	0.0007911	5.17	0.288561
C12	4537300	5.15	0.0005278	19.08	2.99021
D12	4940800	4.94	0.0007484	15.20	8.84450

Mean values of the parameters calculated from experiments B12, C12 and D12:

	A_0	a
$k' = A_0\exp(-at)$	4716413	0.0018685
$k' = A_0[1/(1+at)]$	5049359	0.0029293
$k' = A_0[1/(1+at)]^2$	4865081	0.0011514
$k' = A_0[1/(1+at)]^3$	4812259	0.0007138

[a]Units $(dm^3)^{n+m+p+q}\ kg^{-1}\ s^{-1}\ mol^{-(n+m+p+q-1)}$. [b]Units h^{-1}.

much slower. These results are in agreement with those presented in the literature.[11,24,25]

The kinetics of the catalyst deactivation was determined using eqn. (3), where E/R, n, m, p and q were fixed to the values determined in the Reaction Kinetics section ($E/R = 9598$ K, $n = 0.74$, $m = 0.47$, $p = -0.18$ and $q = 0$) and k' was determined from each experiment using the obtained conversion vs. reactor bed length data. The k' obtained was plotted against the catalyst age, and several models of deactivation were tested. The models used were $k' = A_0\exp(-at)$ (exponential model) and $k' = A_0[1/(1+at)]^n$ (hyperbolic model), where n is 1, 2 or 3. The parameter values A_0 and a were determined using the regression program REPROCHE.

Four separate experimental sets were used. In experiment A10 (Table 2), the inlet temperature (T_0) was 575 K and and the space velocity (S) was 791 h^{-1}. Conversion and temperature data from different reactor length coordinates were collected ten times between 73 and 400 h of operation. In experiments B12, C12 and D12 (Table 2), the space velocity was 1997 h^{-1}, but the inlet temperatures were different: 600 K (B12), 625 K (C12) and 650 K (D12). In experiment B12, the samples were taken eight times between 87 and 262 h, in experiment C12, five times between 90 and 366 h and in experiment D12, nine times between 28 and 404 h.

The parameter values obtained from each experiment are shown in Table 2. According to statistical analysis the best fit is obtained with the hyperbolic model $k' = A_0[1/(1+at)]$. Two examples of the experimental data and the estimated k' profiles are shown in Figs. 3a and 3b.

The mean parameter values of models were calculated from experiments B12, C12 and D12 (Table 2). The best fit was obtained when a hyperbolic model with $n = 1$ was used. The parameter values obtained were $A_0 = 5.0494\times10^6$ $(dm^3)^{1.03}\ mol^{-0.03}\ kg^{-1}\ s^{-1}$ and $a = 2.9293\times10^{-3}\ h^{-1}$.

The surface area, pore volume and pore radius were obtained from the N_2 condensation measurements, which are reliable for small pores with diameters between 1.0 and 40 nm. The surface area, average pore radius and pore volume of a fresh iron oxide/chromium oxide catalyst were $S_{BET} = 53.2\ m^2\ g^{-1}$, $r_{aver} = 5.1$ nm and $V_{tot} = 0.137\ cm^3\ g^{-1}$, respectively. The corresponding values for a catalyst which was exposed for 430 h to a process gas with a maximum

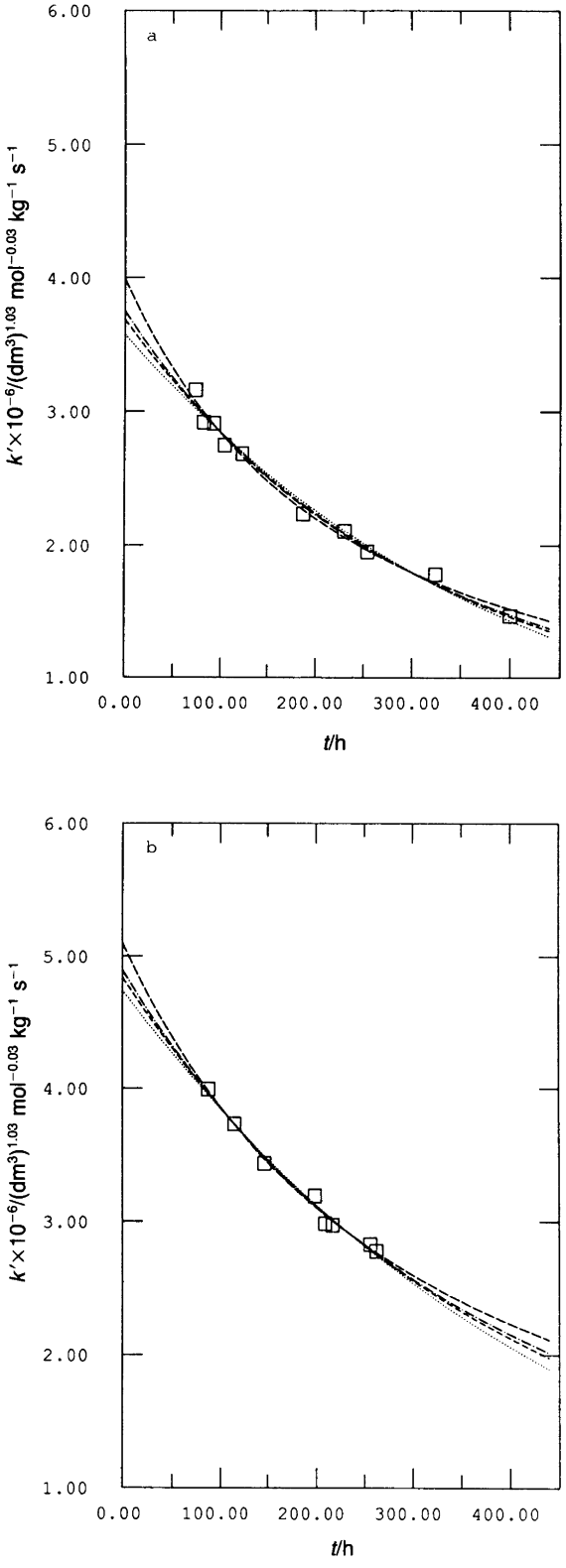

Fig. 3. Experimental and estimated k' profiles for (a) experiment A10, (b) experiment B12 (Table 2): (□) experimental values, (···) $k' = A_0 \exp(-at)$, (– – –) $k' = A_0[1/(1+at)]$, (–·–·) $k' = A_0[1/(1+at)]^2$, and (- - - -) $k' = A_0[1/(1+at)]^3$.

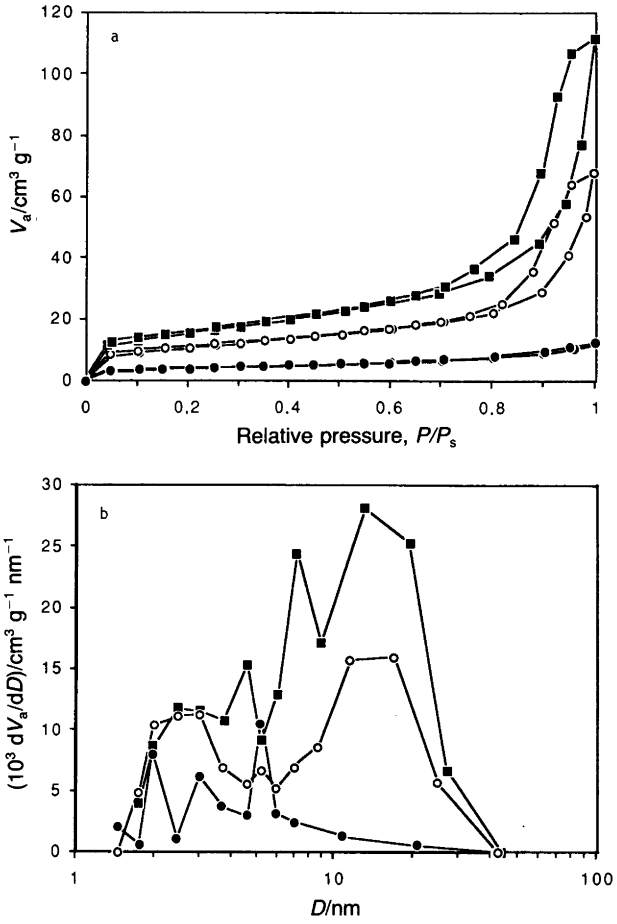

Fig. 4. (a) Nitrogen adsorption/desorption isotherms and (b) pore size distributions for iron oxide/chromium oxide catalysts measured by N_2 adsorption: (■) a fresh catalyst, (○) a catalyst used in process gas at 300–450 °C for 430 h and (●) a catalyst used in process gas at 300–600 °C for 250 h.

temperature of 450 °C were S_{BET} = 35.5 $m^2\ g^{-1}$, r_{aver} = 6.0 nm and V_{tot} = 0.104 $cm^3\ g^{-1}$. If the catalyst was exposed to a higher temperature (up to 600 °C) a further decrease of the surface area and pore volume was observed: S_{BET} = 15.9 $m^2\ g^{-1}$ and V_{tot} = 0.027 $cm^3\ g^{-1}$. The nitrogen adsorption/desorption isotherms and pore size distribution curves for the catalysts are shown in Figs. 4a and 4b.

The mercury penetration method was used to determine the pore size distribution of the larger pores. The pore size distributions for one fresh and two used catalysts measured by N_2 condensation and Hg penetration methods are shown in Fig. 5. The pore size distribution seems to move towards larger pore radii during the reaction. Smaller pores are probably aggregated into larger pores. The decrease in the amount of smaller pores, with the corresponding decrease in the catalytic activity, indicates that pores smaller than 38 nm contribute most to the shift reaction.

For comparison, the pore size distribution of a catalyst which had been in industrial use over 2 years was mea-

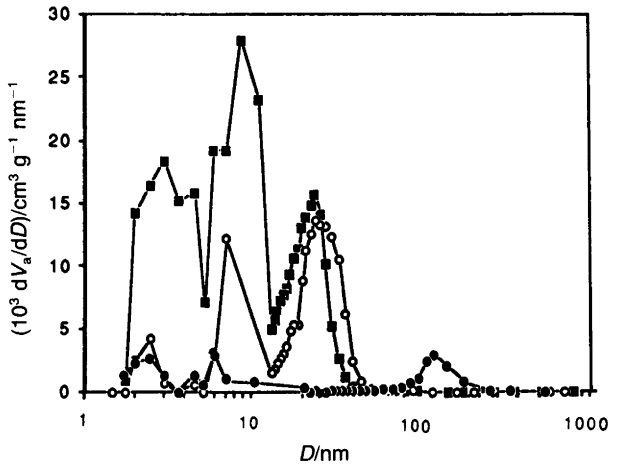

Fig. 5. The pore size distributions for one fresh and two used iron oxide/chromium oxide catalysts using the N_2 adsorption and the Hg penetration methods; (■) a fresh catalyst, (○) a catalyst used in process gas at 300–400 °C for 430 h and (●) a catalyst used in an industrial plant over 2 years.

sured. The small pores had completely disappeared; the typical pore sizes were between 90 and 200 nm (Fig. 5). This observation is in accordance with the literature: it is claimed[26] that all pores of a completely deactivated catalyst have diameters above 50 nm, which corresponds to the pore size of magnetite.

The deactivation of the iron oxide/chromium oxide catalyst may also be caused by coke formation. Therefore, some fresh and used catalysts were analyzed by scanning electron microscopy (SEM) and photoelectron spectroscopy (XPS). According to these analyses both fresh and used catalyst samples contained carbon species, and the amount of carbon on the surface had not increased during the use. So, the carbon formation during the process seems to be negligible. Thus, the deactivation is mainly caused by sintering.

Conclusions

The kinetics of the water–gas shift reaction and the deactivation of the iron oxide/chromium oxide catalyst were studied. A non-isothermal approach for packed bed reactor modelling was applied to determine the parameters of the power law kinetic equation [eqn. (3)] and of the exponential and hyperbolic models of the catalyst deactivation (Table 2).

The non-isothermal approach involving the direct use of the experimental temperature profiles in the component continuity equation proved to be a useful method for technical kinetic studies. The kinetic parameters obtained were in good agreement with those obtained in isothermal conditions by other workers.

The reduction in the catalyst activity was best described by a hyperbolic model. The deactivation was found to be due to a sintering process. The decrease in the catalyst activity was linked to a decrease in the pore volume. Deactivation caused by coke formation could be excluded according to the SEM and XPS analyses.

Nomenclature

A_0	parameter in the deactivation model, $(dm^3)^{1.03}$ $mol^{-0.03}$ kg^{-1} s^{-1}
a	parameter in the deactivation model, h^{-1}
c	concentration, mol dm^{-3}
D	pore diameter, nm
E	activation energy, kJ mol^{-1}
ΔH	reaction enthalpy, kJ mol^{-1}
k	rate constant, $(dm^3)^{n+m+p+q}$ $mol^{-(n+m+p+q-1)}$ kg^{-1} s^{-1}
k'	frequency factor, $(dm^3)^{n+m+p+q}$ $mol^{-(n+m+p+q-1)}$ kg^{-1} s^{-1}
K	equilibrium constant
L	reactor length coordinate, dm
m	concentration exponent of H_2O
MRS	mean residual square
n	concentration exponent of CO
$\dot{n}_{CO}$	molar flow rate of CO, mol h^{-1}
p	concentration exponent of CO_2
P_s	saturation pressure of gas at liquid nitrogen temperature, mmHg
P	measured pressure in N_2 adsorption measurements, mmHg
q	concentration exponent of H_2
r	rate, mol g^{-1} s^{-1}
R	gas constant, = 8.314 J K^{-1} mol^{-1}
r_{aver}	average pore radius, nm
s	estimated standard deviation
S	space velocity, h^{-1}
S_{BET}	the BET surface area, m^2 g^{-1}
ΔS	reaction entropy, J K^{-1} mol^{-1}
T	temperature, K
t	time, h
V	volume of the catalyst bed, dm^3
V_a	volume of gas adsorbed, cm^3 g^{-1}
V_{tot}	total catalyst pore volume, cm^3 g^{-1}
X	conversion
β	reversibility factor, $\beta = (c_{CO_2}c_{H_2})/(c_{CO}c_{H_2O}K)$
ϱ_b	catalyst bulk density, g cm^{-3}

Acknowledgements. This work is a part of the Computer Aided Reactor Design (CARD) project financed by The Technology Development Center (TEKES). The financial support given to one of the authors (R. Keiski) from The Academy of Finland, Acta Chemica Scandinavica, Emil Aaltosen Säätiö and *Teollisen Kulttuurin Tutkimussäätiö* are gratefully acknowledged.

References

1. Newsome, D. S. *Catal. Rev. Sci. Eng. 21* (1980) 275.
2. Keiski, R. L. *Kem.-Kemi 12* (1985) 465.
3. Mars, P. *Chem. Eng. Sci. 14* (1961) 375.
4. Moe, J. M. *Chem. Eng. Progr. 58* (1962) 33.
5. Bohlbro, H. *J. Catal. 3* (1964) 207.

6. Kulkova, N. V. and Temkin, M. I. *Zh. Fiz. Khim. 23* (1949) 695.
7. Hulburt, H. M. and Vasan, C. D. S. *AIChE J. 7* (1961) 143.
8. Puri, V. K., Mahapatra, H., Kursetji, R. M., Ganguli, N. C. and Sen, S. P. *Technol. 10* (1973) 224.
9. Bohlbro, H. *An Investigation on the Kinetics of the Conversion of Carbon Monoxide with Water Vapour over Iron Oxide Based Catalysts,* Gjellerup, Copenhagen 1969.
10. Chandra, M., Singh, S. S., Sinha, A. K., Sinha, N. K., Banerjee, B. and Ghosal, S. R. *Technol. 10* (1973) 208.
11. Hoque, S. N., Ghorai, D. K., Mehta, N. C., Sen, B. and Bhattacharyya, N. B. *Fertilizer Technol. 14* (1977) 381.
12. Kontsevoi, A. L., Zhidkov, B. A., Chipiga, G. P. and Popik, I. V. *Kinet. Katal. 14* (1976) 72.
13. Hoogschagen, J. and Zwietering, P. *J. Chem. Phys. 21* (1953) 2224.
14. Keiski, R. L., Salmi, T. and Pohjola, V. J. *Extended Abstracts of the AIChE 1989 Spring National Meeting,* April 2–6, 1989, AIChE, Houston, TX 1989.
15. Gregg, S. J. and Sing, K. S. *Adsorption, Surface Area and Porosity,* Academic Press, London 1967.
16. Härkönen, M. *Surface Area and Chemisorption Analysis of Raney Nickel,* Report 82, University of Oulu, Oulu, Finland 1982.
17. Lowell, S. *Introduction to Powder Surface Area,* John Wiley & Sons, New York 1979.
18. Vajda, S. and Valko, P. *Reproche, Regression Programs for Chemical Engineers,* Eurecha Manual, Budapest 1985.
19. Michelsen, M. L. *AIChE J. 22* (1976) 594.
20. Bohlbro, H. and Jorgensen, M. H. *Chem. Eng. World 5* (1970) 46.
21. Goodridge, F. and Quazi, H. A. *Trans. Inst. Chem. Eng. 45* (1967) T274.
22. Podolski, W. F. and Kim, Y. G. *Ind. Eng. Chem., Process Des. Dev. 13* (1974) 415.
23. Salmi, T., Lindfors, L.-E. and Boström, S. *Chem. Eng. Sci. 41* (1986) 929.
24. Chandra, M., Singh, S. S., Banerjee, B., Sinha, A. K. and Sinha, N. K. *Technol. 9* (1972) 358.
25. Chinchen, G. C., Logan, R. H. and Spencer, M. S. *Appl. Catal. 12* (1984) 89.
26. Ray, A. M., Yadav, B., Roy, A. K., Sen, B. and Roy, H. C. *Ind. J. Technol. 25* (1987) 61.

Received November 27, 1989.